Materials Letters 115 (2014) 268–271

Contents lists available at ScienceDirect

Materials Letters

journal homepage: www.elsevier.com/locate/matlet

Developing thermodynamic stability diagrams for equilibrium-grain-size binary alloys

Naixie Zhou, Jian Luo*

Department of NanoEngineering, Program of Materials Science and Engineering, University of California, San Diego; La Jolla, CA 92093-0448, USA

ARTICLE INFO

Article history:
Received 3 September 2013
Accepted 22 September 2013
Available online 25 October 2013

Keywords:
Computational thermodynamics
Grain boundary
Materials Genome
Nanocrystalline alloy

ABSTRACT

Bulk computational thermodynamics are extended to model binary poly/nanocrystalline alloys by incorporating grain boundary energies computed by a multilayer adsorption model. A new kind of stability diagram for equilibrium-grain-size poly/nanocrystalline alloys is developed. Computed results for Zr-doped Fe are validated by prior experiments and provide new physical insights regarding stabilization of nanoalloys and its relation to solid-state amorphization. This work supports a major scientific goal of extending bulk computational thermodynamics methods to interfaces and nanomaterials and developing relevant thermodynamic stability diagrams as extensions to bulk phase diagrams, which can be useful new tools for the "Materials Genome" initiative.

1. Introduction

In 1993, Weissmüller [1,2] reported a theory of thermodynamic stabilization of nanocrystalline alloys, and this theory was further elaborated by Kirchheim et al. [3,4]. It was proposed that the thermodynamic driving force for grain growth can be reduced by reducing GB energy (γ_{GB}) via GB segregation (*a.k.a.* adsorption). A nanocrystalline alloy can be stabilized as the effective γ_{GB} approaches zero. Subsequent experiments have been conducted to seek for stabilized nanocrystalline alloys in Fe–Zr [5,6], Pd–Zr [7], and other systems [8–10]. In these systems, the "stable" nanocrystalline alloys typically represent *metastable states* in supersaturated regions occurring when precipitation is hindered kinetically. This is consistent with Kirchheim's analysis [3]. Recently, Schuh and co-workers developed a "Regular Nanocrystalline Alloy" model and analyzed systems with positive pair-interaction parameters [11–13]. Saber et al. refined this model by incorporating both chemical and elastic segregation enthalpies [14], which was also an extension of their earlier model of ferrous alloys [15]; both models used a simplified monolayer/bilayer version of the Wynblatt–Ku type segregation formulation [16]. This work further combines a calculation of phase diagrams (CALPHAD) analysis with a more realistic Wynblatt–Chatain type multilayer segregation (complexion) model [16] to simulate stable, metastable and unstable regions of polycrystalline binary alloys systematically for multiple phase fields, providing new quantitative insights regarding the competitions and underlying relations among precipitation, stabilization of nanoalloys, and solid-state amorphization.

A further scientific goal of this study is to develop new thermodynamic stability diagrams (as extensions to bulk phase diagrams) as novel materials design tools. In a boarder content, phase diagrams, along with CALPHAD methods [17], are arguably amongst the most useful tools for materials design. It is now well-established that the thermodynamic stability of an interface or a nanoscale system that has a large amount of interfaces can drastically differ from that of a bulk material. As an example, nanoparticles can often melt at hundreds of degrees below the bulk melting temperature [18]; along this line, Tanaka et al. extended CALPHAD methods to compute phase diagrams for nanoparticles of binary alloys [19,20]. In another relevant study, researchers demonstrated that nanometer-thick, impurity-based, liquid-like films can be stabilized at grain boundaries (GBs) well below the bulk solidus lines [21–23]. Further studies extended the bulk CALPHAD methods to predict the stability of such liquid-like intergranular films (which can be considered as an "interfacial phase" and named as "complexion" to differentiate them from bulk phases [24–29]) and such GB diagrams are proven useful for forecasting activated sintering and designing sintering protocols [30–33]. This series of recent studies collectively point us to a potentially-transformative research direction of extending bulk CALPHAD methods to interfaces and nanomaterials with a large amount of interfaces; some research efforts in this area are also reviewed by Kaptay [34]. This work represents another such new endeavor of modeling equilibrium-grain-size poly/nanocrystalline alloys by incorporating GB energies in thermodynamic modeling.

It is important to differentiate two possible types of thermodynamic stability diagrams that may be developed for nanomaterials.

---

* Corresponding author. Tel.: +1 858 246 1203; fax: +1 858 534 9553.
E-mail address: jluo@alum.mit.edu (J. Luo).

0167-577X/$ - see front matter © 2013 Elsevier B.V. All rights reserved.
http://dx.doi.org/10.1016/j.matlet.2013.09.093

The first type of diagrams represent the shifts in phase boundaries given a constraint of artificially-fixed sizes (e.g., particle or grain sizes); Tanaka et al.'s studies of binary nanoparticles [19,20] belong to this type. The current study aims to develop the second type of stability diagrams to model the thermodynamic stability of equilibrium-grain-size poly/nanocrystalline alloys without imposing pre-selected (kinetically-determined) grain sizes. Fe–Zr is selected as our modeling system because of the existence of both thermodynamic data [35] and experimental results [5,6,36], and our goal is to develop models and methods that can be extended to other systems. In the current (first) study, we model a binary poly/nanocrystalline alloy (of equiaxed grains) for which experimental data exist for validation. Our ultimate goal is to further extend the methods to multicomponent alloys, where they can have more impacts (similar to bulk CALPHAD methods).

2. Modeling methods

At constant pressure and temperature, the molar free energy of a polycrystalline binary alloy A–B (A = Fe and B = Zr for our specific case) can be written as

$$G_m = (1-X)\mu_A + X\mu_B + \overline{A_{GB}}\gamma_{GB}, \tag{1}$$

where X is the overall composition (atomic fraction) of the solute B, μ_A and μ_B are chemical potentials, $\overline{A_{GB}}$ is the GB area per mole of atoms, and γ_{GB} is the GB energy. When the grain size is small, the overall composition (X) differs from the bulk/crystal composition (X_C, inside the grain) because of GB segregation; the mass conservation law specifies

$$X \approx X_C + \overline{A_{GB}}\Gamma, \tag{2}$$

where Γ is the GB excess of solute. Recent observations of the increased apparent solubility of dopants in nanocrystalline ZnO [37] and steels [38,39] are likely due to that X can be substantially greater than X_C for nano-grained materials. Under the condition of a kinetically-limited (fixed) grain size, the changed solubility can also be partially related to a shift in the X_C value (in equilibrium with the secondary phase) due to the added $\overline{A_{GB}}\gamma_{GB}$ term in Eq. (1); this effect should be modeled by the first type of stability diagrams (with per-selected grain sizes) discussed above, which is beyond the scope of this letter.

In this study, we adapt the Wynblatt–Chatain multilayer segregation (complexion) model [16] to consider general twist GBs in a BCC alloy; the following expression is derived by adapting the Wynblatt–Chatain equations [16] (with two modifications: we assume $J_{max} = 1$ or all broken bonds exist in the first layer since we adopt a general twist (110) GB to represent the general GBs in Fe; we also adjusted the in-plane and vertical coordinate numbers since the original Wynblatt–Chatain model is for FCC alloys):

$$\begin{aligned}\gamma_{GB} = \min\Bigg\{ & (p-1)z_v N\left[2X^1_{GB}(1-X^1_{GB})\omega + X^1_{GB}e_{BB} + (1-X^1_{GB})e_{AA}\right] \\ & - 2N\sum_{i=1}^{+\infty}\left[X^i_{GB}\Delta E^i_{els}\right] + 2N\omega\sum_{i=1}^{+\infty}\left[-z(X^i_{GB}-X_C)^2 + z_v(X^i_{GB}-X^{i+1}_{GB})^2\right] \\ & + 2NkT\sum_{i=1}^{+\infty}\left[X^i_{GB}\ln\left(\frac{X^i_{GB}}{X_C}\right) + (1-X^i_{GB})\ln\left(\frac{1-X^i_{GB}}{1-X_C}\right)\right]\Bigg\},\end{aligned} \tag{3}$$

where X^i_{GB} is the composition in the ith layer near the GB core, e_{AA}, e_{BB}, and e_{AB} are bonding energies ($e_{FeFe} = -1.07$ eV/bond and $e_{ZrZr} = -1.56$ eV/bond, which are estimated from atomization enthalpies [40]. The energy difference between the HCP and BCC phase for Zr is corrected by using CALPHAD data [35]), $\omega\,[\equiv e_{AB} - 0.5(e_{AA} + e_{BB})]$ is the pair-interaction parameter (estimated to be -0.025 eV/bond for Fe–Zr from the CALPHAD data [35]), z is the total coordinate number ($z = 8$ for BCC), z_v is the coordination number above the plane ($z_v = 2$ for a BCC twist (110) GB), p (the fraction of reconnected bonds) is set to be 5/6 to represent a "general GB" so that the GB energy is 1/3 of the surface energy for a pure element, N is the number of the lattice sites per unit area, k is the Boltzmann constant and T is temperature. ΔE^i_{els} is the elastic energy in the ith layer, which decreases exponentially with the distance to the GB core (h^i) according to $\Delta E^i_{els} = \Delta E^1_{els}\exp[-1.01(h^i/r_B)^{1.53}]$, where r_B is the atomic radius of B; ΔE^1_{els} is given by the Friedel model [16], which is calculated to be 0.96 eV/atom for Fe–Zr. The equilibrium GB adsorption profile can be obtained by minimizing Eq. (3) ($\partial\gamma_{GB}/\partial X^i_{GB} = 0$), leading to a McLean type adsorption equation for each layer:

$$\frac{X^i_{GB}}{1-X^i_{GB}} = \frac{X_C}{1-X_C}\exp\left(-\frac{\Delta H^i_{seg}}{RT}\right) \tag{4}$$

Here, ΔH^i_{seg} is the adsorption enthalpy of the ith layer and its specific expression is given in Ref. [16]. Eqs. (3) and (4), along with the adsorption profile $(X_{GB}{}^i)_{i=1,\,2,\ldots}$ that minimizes Eq. (3), can be solved efficiently via an iterative method. The GB excess of solute is given by $\Gamma \approx 2N\sum_i(X^i_{GB} - X_C)$.

3. Results and discussion

Fig. 1 shows several computed normalized GB energy ($\gamma_{GB}/\gamma_{GB}{}^{(0)}$) and GB excess of solute (Γ) vs. bulk composition (X_C) curves. Here, $\gamma_{GB}{}^{(0)}$, the GB energy for pure Fe, is computed from Eq. (3) to be ~ 1 J/m^2, which is consistent with the measured value [41]. In a binary alloy, GB adsorption reduces GB energy according to

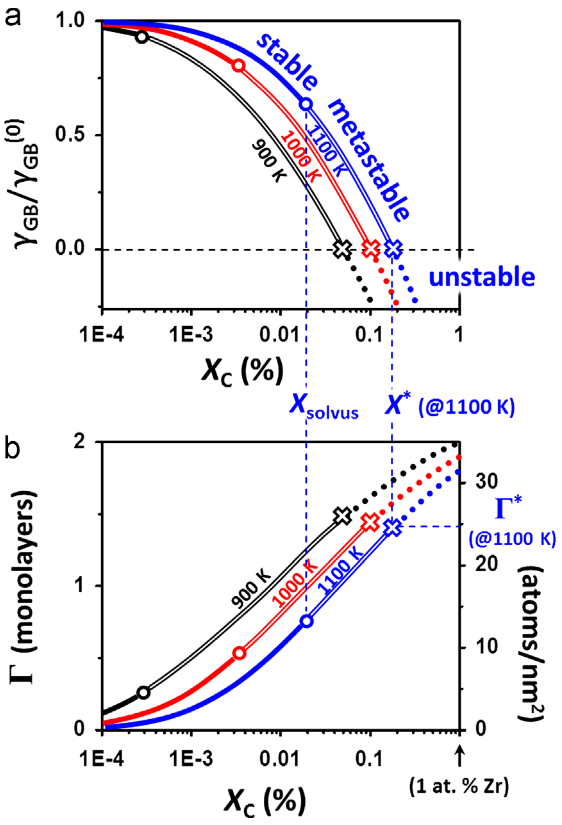

Fig. 1. Computed (a) normalized GB energy ($\gamma_{GB}/\gamma_{GB}{}^{(0)}$) and (b) GB excess of the solute (Γ) vs. bulk composition (X_C) curves for Zr-doped Fe. The stable, metastable, and unstable regions, respectively, are represented by the solid, double, and dotted lines, respectively.